Photochemistry and Photobiology, 2013, 89: 1273–1282

Invited Review

Effect of Concentration on the Photophysics of Dyes in Light-Scattering Materials†

Hernán B. Rodríguez[1] and Enrique San Román*[2]

[1]INIFTA, Facultad de Ciencias Exactas, Universidad Nacional La Plata, Argentina
[2]INQUIMAE / DQIAyQF, Facultad de Ciencias Exactas y Naturales, Universidad de Buenos Aires, Argentina

Received 15 April 2013, accepted 22 May 2013, DOI: 10.1111/php.12107

ABSTRACT

Photoactive materials based on dye molecules incorporated into thin films or bulk solids are useful for applications as photosensitization, photocatalysis, solar cell sensitization and fluorescent labeling, among others. In most cases, high concentrations of dyes are desirable to maximize light absorption. Under these circumstances, the proximity of dye molecules leads to the formation of aggregates and statistical traps, which dissipate the excitation energy and lower the population of excited states. The search for enhancement of light collection, avoiding energy wasting requires accounting the photophysical parameters quantitatively, including the determination of quantum yields, complicated by the presence of light scattering when particulate materials are considered. In this work we summarize recent advances on the photophysics of dyes in light-scattering materials, with particular focus on the effect of dye concentration. We show how experimental reflectance, fluorescence and laser-induced optoacoustic spectroscopy data can be used together with theoretical models for the quantitative evaluation of inner filter effects, fluorescence and triplet formation quantum yields and energy transfer efficiencies.

INTRODUCTION

Light collection efficiency is crucial for the development of photoactive materials based on dye molecules incorporated into thin films or bulk solids for applications such as photosensitization, photocatalysis, solar cell sensitization and fluorescent labeling, among others. A way to extend the light harvesting efficiency consists in working at high concentrations with highly absorbing dye molecules covering a broad spectrum from the UV to IR. Unfortunately, most highly absorbing dyes are planar molecules prone to aggregate or build up energy traps at high concentrations leading to concentration self-quenching and energy wasting.

The design of photosensitizers based on the attachment of dyes to soluble (1,2) or insoluble (3,4) polymeric materials has been addressed in the literature. Dyes can be grafted on the surface of particles with the aim of producing fluorescence labeling agents (5,6). A general observation is the decrease in fluorescence intensity and the shortening of the excited-state lifetime as dye concentration increases due to self-quenching. An interesting example is the use of polymers as drug delivery agents for photodynamic therapy (7,8). A suitable polymer is labeled with a dye capable of photogenerating singlet molecular oxygen or other reactive oxygen species. Due to self-quenching, the conjugate is not photoactive until it enters the target cells, where enzymatic attack liberates the dye, thus recovering photoactivity.

Most of the reported examples are based on single, randomly distributed dyes, although the supramolecular arrangement of multiple dyes on a single supporting material has been addressed (9). Relay dyes have been used to increase power conversion efficiency in dye-sensitized solar cells (10,11). A zinc phthalocyanine was used as sensitizing dye of TiO_2 and different blue-absorbing dyes dissolved in the electrolyte transferred energy to the sensitizing dye. The same authors developed a model to evaluate energy transfer efficiencies from the relay to the sensitizing dye in a porous film, accounting for dynamical quenching and dye diffusion (12). Much rests to be done, however, to obtain reliable and robust devices.

Light-scattering layers of polycrystalline anatase are sometimes introduced in dye-sensitized solar cells to enhance light absorption (13). However, light scattering is in general considered as a drawback to evaluate absolute efficiencies because the fraction of excitation radiation absorbed by the sample is difficult to compute. When light scattering is not severe, extinction spectra are measured in a transmission spectrophotometer subtracting the scattering background to obtain absorption spectra. However, measurements performed at different positions inside the spectrophotometer cell compartment yield usually different results. To circumvent this problem, Martini *et al.* (14) used a reference with the same scattering properties as the sample. They assumed that the fluorescence quantum yield of the reference is the same as in solution, but this is certainly not a general rule. Determination of absorption spectra and fluorescence quantum yields in the presence of light scattering has been further discussed by Gaigalas *et al.* (15,16).

The cases given above are just a few examples on the problematic encountered when dealing with materials containing dyes at high concentrations, particularly when light scattering is present. V. Ferreira *et al.* (17) addressed some time ago the spectroscopy of organic surfaces modified with organic dyes, including aspects of the photophysics of light-scattering particulate solids. We review here the photophysics of dyes in light-scattering materials, with emphasis in the determination of luminescence and triplet

*Corresponding author email: esr@qi.fcen.uba.ar (Enrique San Román)
†This article is part of the special issue dedicated to the memory of Elsa Abuin.

quantum yields and excitation energy transfer and trapping efficiencies and the effect of dye concentration on these properties. In the following sections, techniques currently used for the determination of **Photoluminescence Quantum Yields** are summarized, addressing in particular **Integrating Sphere Methods**. The problem of **Reabsorption and Reemission of Fluorescence** is discussed in detail, especially for optically thick systems. The following sections cover **Molecular Interactions and Non-radiative Energy Transfer** and the **Determination of Quantum Yields by Laser Induced Optoacoustic Spectroscopy**. Finally, the section on **Experimental Results** summarizes mainly our own experience in the field.

PHOTOLUMINESCENCE QUANTUM YIELDS

The photoluminescence quantum yield, Φ, is currently defined for a single emitter as the fraction of molecules that emit a photon of a particular kind—fluorescence, phosphorescence—after excitation by absorption of light (18). The prompt fluorescence quantum yield, Φ_F, is a theoretical quantity equivalent to the quotient between the fluorescence rate constant and the sum of the rate constants of all processes depopulating the singlet excited state. The phosphorescence quantum yield, Φ_P, is related to rate constants involving the singlet and the triplet state. In particular, $\Phi_P = \Phi_T \times \eta_P$, where Φ_T is the triplet quantum yield and η_P is a phosphorescence efficiency, *i.e.* the quotient between the phosphorescence rate constant and the sum of the rate constants of all processes depopulating the triplet excited state. Quantum efficiency or simply efficiency, a term otherwise used as a synonym of quantum yield, is defined here as a measure of the relative rate of a given reaction step involving some species with respect to the sum of the rate constants of all processes depopulating that species (19).

The actual measurement of photoluminescence quantum yields involves the quotient between the number of photons emerging and the number of photons absorbed by the sample, *i.e.* a technical or observed quantity, Φ_{obs}. In general, this quantity differs from Φ. Aside from the presence of any other molecule (*e.g.* an impurity), solvent or supporting material that could interfere at the absorption or emission wavelengths, other effects become important as the concentration of the species under consideration increases, mainly ground-state molecular aggregation, the formation of emitting or dark excimers and excitation and emission inner filter effects. To avoid these effects in solution, spectroscopic grade solvents and highly dilute emitters are used. In the limit of infinite dilution, $\Phi_{obs} = \Phi$ and the emission intensity becomes proportional to the sample absorbance, which in turn depends linearly on the emitter concentration.

The occurrence of inner filter effects in homogeneous transparent samples, extensively discussed in the current literature involving solution studies (20), leads to a dependence of the observed emission spectrum and quantum yield on the optical arrangement of the measuring system (front face, right angle, transmission), on the absorbance of the sample and on the location of the detector (21). Birks analyzed in detail the corrections needed for different measurement geometries in solution (22). Scattering materials as turbid suspensions or thin films pose additional difficulties for the determination of photoluminescence quantum yields, making measurements strongly dependent on geometry. Another limitation encountered when dealing with light-scattering materials is the lack of emission standards and the corresponding need of absolute methods as those to be described in the next paragraphs.

Wrighton *et al.* (23) and Liu *et al.* (24) performed photoluminescence quantum yield measurements on powders using a conventional emission spectrometer. In the first case, an optically thick sample, for which light is either reflected or absorbed and transmission is negligible, was used. The sample was excited normally with monochromatic light and emission was collected from the front face with a mirror at an arbitrary angle. Most important is that specular reflectance is excluded and the same fraction of diffuse reflectance and luminescence are measured. It was assumed that the angular distribution of diffuse and emitted light is the same, *i.e.* the surface is Lambertian (25). Ware and coworkers measured semitransparent samples and, to avoid light leakage, they used a U-shaped mirror to contain the sample. The excitation beam was passed in some experiments through a diffuser plate to illuminate the sample evenly. It was assumed that emission is ideally diffused. Essentially, both methods are based in the relationship:

$$\Phi_{obs} = \frac{J_E}{J_0 - J_S} \tag{1}$$

where J_E is the area below the emission spectrum and J_S and J_0 the areas of the radiation scattered by the sample and a suitable, nonabsorbing blank respectively. As in both examples transmittance is made negligible, J_0–J_S is proportional to the absorbed intensity. These methods can be applied when the excitation band and the emission spectrum do not overlap. A common drawback is that, whereas J_S and J_0 present a strong and narrow band limited by the entrance slit of the excitation monochromator, J_E has a weak and a broad spectrum. Therefore, detector linearity is required over a broad dynamic range. Spectra must be corrected for the wavelength dependence of the fluorimeter emission channel.

INTEGRATING SPHERE METHODS

A way to account for nonideality of the light-scattering material is the usage of integrating spheres inside the spectrofluorometer cavity. This approach was also used by Liu *et al.* (24). The sample and the nonabsorbing blank were sealed into quartz or glass tubes located one at a time at the center of the sphere. The photoluminescence quantum yield was again calculated through Eq. (1). de Mello *et al.* (26), using also an integrating sphere and laser irradiation, performed three measurements, the beam impinging: (1) on the inner surface of the empty sphere; (2) on the inner surface of the sphere containing the sample; and (3) on the sample contained in the sphere respectively. The output of the sphere was fed into a CCD camera through an optical fiber to obtain the corresponding spectra. From these measurements the fraction of laser light absorbed by the sample and the photoluminescence quantum yield were obtained. For the calculation to be valid, reabsorption of the emitted radiation by the sample should be negligible, *i.e.* the absorption and the emission spectra should not overlap. Again, detector linearity over a large intensity range is required.

The methods already described make use of an emission spectrometer. The determination of photoluminescence quantum yields of light-scattering materials can also be afforded using a standard double beam integrating sphere reflectance spectrophotometer. The sample and a nonabsorbing reference are located as usual outside the sphere. The method, suited for optically thick

particulate samples, was simultaneously developed by Mirenda *et al.* (27) and Vieira Ferreira *et al.* (28), and consists in comparing diffuse reflectance values obtained with and without an optical filter interposed between the sphere and the photomultiplier detector. The filter has to block a substantial fraction of the sample luminescence. The true diffuse reflectance, *i.e.* the reflectance devoid of emission artifacts, is also obtained. According to ref. (27):

$$\Phi_{obs} = \frac{R_{d,obs}(\lambda_0) - R^f_{d,obs}(\lambda_0)}{I(\lambda_0)\cdot[1 - R^f_{d,obs}(\lambda_0)] - I^f(\lambda_0)\cdot[1 - R_{d,obs}(\lambda_0)]} \quad (2)$$

$$R_d(\lambda_0) = \frac{I(\lambda_0)\cdot R^f_{d,obs}(\lambda_0) - I^f(\lambda_0)\cdot R_{d,obs}(\lambda_0)}{I(\lambda_0) - I^f(\lambda_0)} \quad (3)$$

$$I(\lambda_0) = \int_\lambda f_{obs}(\lambda)\frac{s(\lambda)}{s(\lambda_0)}\frac{\lambda_0}{\lambda}d\lambda \quad (4)$$

$$I^f(\lambda_0) = \int_\lambda f_{obs}(\lambda)\frac{T(\lambda)}{T(\lambda_0)}\frac{s(\lambda)}{s(\lambda_0)}\frac{\lambda_0}{\lambda}d\lambda \quad (5)$$

where $R^f_{d,obs}$ and $R_{d,obs}$ are the observed diffuse reflectances measured with and without filter, R_d is the true reflectance, $f_{obs}(\lambda)$ is the observed emission spectrum normalized to unit area, s the relative spectral responsivity of the photomultiplier detector, obtained from the spectral responsivity in radiometric units (μA W^{-1}), T the transmittance of the filter and λ_0 and λ the excitation and emission wavelengths respectively. Total reflectances may be used instead of diffuse reflectances. It is assumed that the reflectivity of the integrating sphere and the emission spectrum are independent of the excitation wavelength. The first assumption restricts the application of the method to the visible region unless a calibration is performed and the detector responsivity is modified accordingly. Calibration is also necessary if it is suspected that the photomultiplier responsivity differs from the average values informed by the provider.

The advantage of using optically thick samples following the methodology described in the last paragraph rests in the easiness with which observed quantum yields can be corrected to obtain values devoid of reabsorption and reemission artifacts (see next section). Furthermore, optical thickness ensures that scattering takes place from the front face exclusively. Films and suspensions show in general complex radiation fields and scatter radiation in all directions, making in-sphere methods mandatory. Correction for reabsorption is difficult to perform in the last cases.

REABSORPTION AND REEMISSION OF FLUORESCENCE

Fluorescence reabsorption is generally difficult to quantify and obscures the evaluation of other concentration quenching mechanisms. The literature shows examples where the role of aggregates as excitation energy traps is demonstrated in systems devoid of reabsorption. Studies of concentration quenching of dyes incorporated into vesicles (29), liposomes (30), micelles (31) and nanoparticles (32) have attracted the attention of researchers because these systems may act as dye vehicles for photodynamic therapy of cancer (33,34) or as fluorescent biological labels (35). In these cases, encapsulation of dyes leads currently to very high local concentrations, in conditions where concentration quenching mechanisms are effective, but at low overall absorbance, thus reducing the problem of fluorescence reabsorption. Much work has also been performed in thin films (36–39), particularly in Langmuir–Blodgett films (40–43). The determination of absolute fluorescence quantum yields is usually not performed in these cases. The evaluation of concentration quenching is instead performed through time-resolved fluorescence studies. Although the presence of aggregates as energy traps (*vide infra*) is currently considered, their concentration and its relationship to the dye analytical concentration are rarely evaluated.

Reabsorption of the emitted light (trivial energy transfer) is a result of a strong overlap between the emission and the absorption spectra of the sample. It is a typical phenomenon for fluorescent compounds characterized by a small Stokes shift. It takes place for film samples inside an integrating sphere and whenever highly absorbing thick samples are used. For films, reabsorption can be reduced by lowering the sample volume or corrected by comparing the emission spectra taken inside and outside the sphere (26). For thick samples the effect is unavoidable. When the absorber and the emitter are the same, fluorescence reabsorption is followed by emission and the cycle is repeated an infinite number of times. Birks (44) developed a model for that case based on a single parameter, P, the probability of reabsorption of an emitted photon:

$$\Phi_{obs} = \frac{\Phi_F(1-P)}{1 - P\Phi_F} \quad (6)$$

Eq. (6) rests on the assumption that the probabilities of emission, *i.e.* the fluorescence quantum yield, Φ_F, and reabsorption, P, are independent of the order of the reabsorption–reemission cycle. This implies in turn that reabsorption leads always to the same emission spectrum, *i.e.* red-edge effects (45) are absent. It is also implicitly assumed that the emitter remains in the same form on increasing its concentration and, particularly, that it does not build up molecular aggregates. The use of optically thick samples for the quantification of photoluminescence quantum yields of light-scattering materials is preferred whenever possible because simple approximate solutions of the problem are obtained as it will be demonstrated in what follows.

The problem was first addressed by Oelkrug and Kortüm (46). Working with their equations one finds for the probability that an emitted photon escapes from the sample:

$$\gamma(\lambda,\lambda_0) = \frac{F(R_0)(1+R_0)(1+R)(1-R_0)^{-1}}{R_0^{-1} + R^{-1} - R_0 - R} \quad (7)$$

where R and R_0 are the diffuse reflectances at the emission wavelength λ and the excitation wavelength λ_0, respectively, and $F(R_0) = (1 - R_0)^2/2R_0$ is the remission or Kubelka–Munk function (47) at λ_0. Independently, using Eq. (6), Lagorio *et al.* found for the same quantity (48):

$$\gamma(\lambda,\lambda_0) = \frac{1}{1+\sqrt{\frac{F(R)}{F(R)+2}}} \times \frac{1}{1+\sqrt{\frac{F(R)[F(R)+2]}{F(R_0)[F(R_0)+2]}}} \quad (8)$$

It may be demonstrated that both equations are equivalent. The function $\gamma(\lambda, \lambda_0)$ is a correction factor for the emission spectrum:

$$f_{obs}(\lambda, \lambda_0) = \gamma(\lambda, \lambda_0) f(\lambda) \quad (9)$$

where $f(\lambda)$ is the emission spectrum devoid of reabsorption and reemission effects (the spectrum obtained from an ideally thin layer of particles). On the other side, the same function can be used to calculate the reabsorption probability in Eq. (6):

$$P = \int_{\lambda} f(\lambda)[1-\gamma(\lambda, \lambda_0)]d\lambda \quad (10)$$

Extension of the theory for a system composed of different compounds absorbing at the excitation wavelength, one of them qualified as the emitter yields the following expression for the observed fluorescence quantum yield (49):

$$\Phi_{obs} = \frac{\Phi_F \alpha_0 (1-P)}{1 - P_E \Phi_F} \quad (11)$$

where α_0 is the fraction of excitation light absorbed by the emitter,

$$P_E = \int_{\lambda} f(\lambda)[1-\gamma(\lambda, \lambda_0)]\alpha(\lambda)d\lambda \quad (12)$$

is the probability that an emitted photon is reabsorbed by the emitter and $\alpha(\lambda)$ is the fraction of the total absorbed radiation received by the same compound. Reabsorption–reemission-corrected fluorescence quantum yields can be obtained reverting Eq. (11), as:

$$\Phi_F = \frac{\Phi_{obs}}{\alpha_0(1-P) + \Phi_{obs} P_E} \quad (13)$$

Eqs. (7)–(13) rest on the following assumptions: (1) the surface of the optically thick sample is Lambertian; (2) the Kubelka–Munk theory (25) holds; (3) the reabsorption probability is the same irrespective of the reemission cycle; and (4) the scattering coefficient of the sample is independent of wavelength. The last assumption is fulfilled for limited wavelength intervals by samples composed of particles with dimensions larger than wavelength.

MOLECULAR INTERACTIONS AND NONRADIATIVE ENERGY TRANSFER

In a rigid environment collisional processes are precluded, but other ways are active for concentration quenching. Molecular aggregates lead generally to static quenching as aggregates may act as traps of the excitation energy. They may be also acceptors in energy transfer processes, enhancing the quenching effect. Currently, aggregation leads to a dependence of the absorption or remission function spectrum with concentration. In certain cases, however, concentration quenching is observed without evidence of spectroscopic changes. It is attributed in these cases to weakly interacting molecular pairs constituting excitation energy traps—statistical traps—resulting from the quasi random distribution of dye molecules (50–53).

Energy transfer mechanisms can be classified as radiative or nonradiative, depending on whether the transfer is mediated by a *real* photon or not. Radiative energy transfer has been considered in the previous section. This type of energy transfer takes place at relatively large absorbances, no matter how long intermolecular distances are. On the other hand, nonradiative energy transfer requires close interaction among donor and acceptor and, for a random distribution of molecules, large local acceptor concentrations. In both cases, strong spectral overlap between donor fluorescence and acceptor absorption is needed. Both energy transfer mechanisms can be dealt with together (54), but the current approach consist in treating them as separate phenomena.

Short-range processes (<10 Å), such as Dexter energy transfer and charge resonance interactions, are dominant when forbidden transitions are involved (*e.g.* triplet–triplet energy transfer). Coulombic interactions, on the other hand, can be long-range (up to 80–100Å) dipole–dipole or medium-range multipolar interactions and are predominant for allowed transitions (55). The relative magnitude of the interaction energy, U, compared with the absorption, $\Delta\omega$, and vibronic, $\Delta\varepsilon$, bandwidth of the interacting molecules allows a distinction between strong ($U \gg \Delta\omega, \Delta\varepsilon$), weak ($\Delta\omega \gg U \gg \Delta\varepsilon$) and very weak ($U \ll \Delta\varepsilon, \Delta\omega$) coupling. The case of strong and weak couplings, where coherent energy transfer between molecules leads to stationary exciton states and excitation energy delocalization can be treated in the frame of exciton theory for molecular aggregates (20,56,57). Strong coupling is responsible for abrupt changes in absorption spectra with increasing concentration.

In the case of very weak coupling, excitation is localized and vibrational relaxation occurs before energy transfer: The transfer process is incoherent, leading to the univocal definition of a transfer rate. In the dipole–dipole approximation it corresponds to the Förster Resonance Energy Transfer (FRET) mechanism (58). At high dye local concentrations, when averaged molecular distances are larger than molecular dimensions, FRET is expected to be the predominant nonradiative energy transfer mechanism. Within the Förster mechanism, the energy transfer efficiency for a single donor–acceptor pair is defined as (59):

$$E_{DA} = \frac{k_{ET}}{k_{ET} + k_D} = \frac{1}{1 + (R/R_0)^6} \quad (14)$$

where k_{ET} is the energy transfer rate constant, k_D the intrinsic deactivation rate constant of the excited donor, R the distance between the donor and the acceptor pair and R_0 the *Förster radius*, *i.e.* the distance at which the energy transfer efficiency is 50%. For an ensemble of donor and acceptor molecules, a distribution of distances and orientations has to be taken into account to evaluate the overall energy transfer efficiency. At low donor concentration—interaction among donor molecules is excluded—an averaged distribution of acceptors around a single donor molecule may be considered as a representation of the ensemble.

Considering a random distribution of molecules fixed in space —diffusion does not operate during the excited-state lifetime—, the evaluation of energy transfer efficiency leads to the general expression (60,61):

$$E_{DA} = 1 - \int_0^{\infty} \exp[-x - \sigma S(x)]\mathrm{d}x \quad (15)$$

$$S(x) = \int_{r_c}^{\infty} \left\{1 - \exp\left[-(R_0/r)^6 x\right]\right\} f(r)\mathrm{d}r \quad (16)$$

where $x = t/\tau$; τ is the excited-state lifetime of donors in the absence of acceptors; σ the surface or volume number density of

acceptors according to the dimensionality of the system; r_c the radius of exclusion around donor molecules, *i.e.* the minimum distance at which an acceptor can be located; $f(r)\mathrm{d}r$ is a volume element whose mathematical expression depends on the dimensionality: $f(r)\mathrm{d}r = 2\pi r\mathrm{d}r$ for 2D and $4\pi r^2\mathrm{d}r$ for 3D. Equation (16) can be solved for $r_c = 0$ yielding more tractable expressions as those found elsewhere (62). These equations are valid for negligible energy migration between donor molecules. In the usual case of small donor Stokes shift, the validity is restricted to low concentrations. Many researchers have tackled the problem of energy migration with different approaches and developed several theoretical models (63–66). The mathematical complexity of these theoretical expressions hinders their practical application. Other approaches are based on computational simulations (67–70). Energy migration between donor molecules generally enhances donor–acceptor transfer efficiencies.

From a practical point of view, nonradiative energy transfer can be included into the reabsorption–reemission-scattering model in a phenomenological way. Consider a donor–acceptor system excited in a spectral region where only donor molecules absorb light. The excited donor can deactivate itself emitting a photon, through intrinsic nonradiative processes or transferring nonradiatively the excitation energy to an acceptor molecule. Emitted light can be reabsorbed both by donors and acceptors or escape out of the system. On the other hand, if the acceptor fluoresces, it can undergo reabsorption and reemission. Figure 1 illustrates these processes for the case of singlet–singlet energy transfer (reverse energy transfer is not considered) (71). Notice that no explicit model is given for the nonradiative transfer efficiency, E_{DA}.

All quantities in Fig. 1 with the exception of E_{DA} can be obtained experimentally from spectroscopic data for optically thick and thin samples (72), in particular:

$$P_{ij} = \int_{\lambda} f^i(\lambda)[1 - \gamma(\lambda, \lambda_0)]\alpha^j(\lambda)d\lambda \tag{17}$$

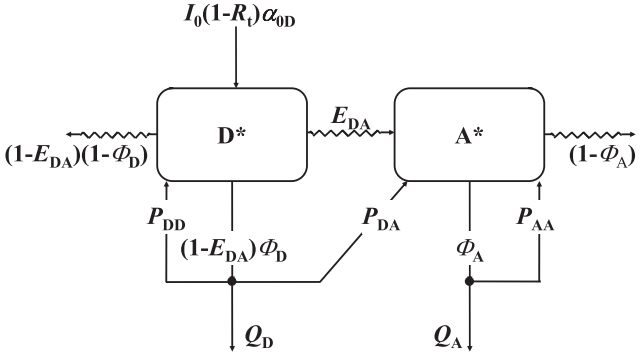

Figure 1. Donor to acceptor radiative and nonradiative energy transfer. From the incident photon flow, a fraction $(1 - R_t)$ is absorbed by the sample and, from this quantity, a fraction α_{0D} excites the donor; $(1 - E_{DA})\Phi_D$ is the effective fluorescence quantum yield of the donor molecule and $(1 - E_{DA})$ $(1 - \Phi_D)$ the probability of intrinsic nonradiative deactivation, such as internal conversion or intersystem crossing, in the presence of nonradiative energy transfer; Q_i and P_{ij} are the probabilities that a photon emitted by species i escapes out of the system or is reabsorbed by species j respectively (see text). Radiative and nonradiative energy transfer from acceptor to donor molecules is excluded (adapted with permission from *Ann. N. Y. Acad. Sci.* **1130**, 247–252).

$$Q_i = \int_{\lambda} f^i(\lambda)\gamma(\lambda, \lambda_0)d\lambda \tag{18}$$

where $f^i(\lambda)$ is the true emission spectrum of species i normalized to unit area over λ, $\alpha^j(\lambda)$ is the fraction of light absorbed by species j at wavelength λ and $\gamma(\lambda, \lambda_0)$ was defined in Eqs. (7) and (8). Until the excitation energy escapes out of the system, either as heat or luminescence, the diagram in Fig. 1 can be traversed by infinite possible paths. The observed fluorescence quantum yields and emission spectra result from considering these paths and their respective probabilities. In this case, the experimentally observed fluorescence quantum yield can be expressed as (72):

$$\Phi_{obs} = \frac{\alpha_0 D}{1 - \Phi_D(1 - E_{DA})P_{DD}} \left\{\Phi_D(1 - E_{DA})Q_D + [\Phi_D(1 - E_{DA})P_{DA} + E_{DA}] \times \frac{\Phi_A Q_A}{1 - \Phi_A P_{AA}}\right\} \tag{19}$$

where Φ_D and Φ_A are the donor and acceptor fluorescence quantum yields, respectively. In the above equations, all the parameters, with the exception of the nonradiative energy transfer efficiency, are accessible from experimental data. Thus, E_{DA} can be readily calculated as a function of the donor and acceptor concentrations. Equation (19) reverts to Eq. (11) for $E_{DA} = 0$ and $\Phi_A = 0$. In that case, $\alpha_{0D} = \alpha_0$, $\Phi_D = \Phi_F$, $P_{DD} = P_E$ and $Q_D = 1 - P$.

The same formalism allows derivation of the expressions for donor and acceptor fluorescence intensities (72). Thus, determination of E_{DA} is also possible from the relative emissions of donor and acceptor. Once the nonradiative energy transfer efficiency is obtained, its dependence on the dye concentrations can be evaluated theoretically in the frame of the proposed energy transfer mechanism.

DETERMINATION OF QUANTUM YIELDS BY LIOAS

Laser-induced optoacoustic spectroscopy has been extensively used for the determination of quantum yields, energies and lifetimes of excited states and reactive intermediates and molecular volume changes in solution (73–76). Also studied were turbid suspensions, gas-phase aerosols, tissue material and biological structures; see ref. (77). In contrast, the application of LIOAS to dry powdered samples has been less frequent owing to the poor acoustic contact and the presence of multiple solid–air interfaces. Recently, a cell suited for this kind of systems and a sample preparation method that allows reproducible measurements was developed for the evaluation of fluorescence quantum yields in light-scattering solids (77). A similar methodology was applied for the determination of triplet quantum yields (78).

In both cases, LIOAS measurements are performed exciting optically thick solid samples in front face using a nanosecond pulsed laser. Samples are prepared applying a controlled pressure during a fixed period of time, using a standardized protocol to achieve reproducible signals. The measurement cell was designed to achieve reproducible acoustic contact between sample and detector, minimizing undesirable effects in thermal and acoustic

conduction. Construction details and sample preparation protocols can be found in ref. (77). Considering optically thick samples and validity of the Kubelka–Munk theory of light scattering, following equations for the ratio between the acoustic signal maximum (H) and the energy of the laser pulse (E) are obtained:

$$\left.\frac{H}{E}\right|_{S} = A(1-R)\left(1-\Phi_{obs}\frac{\langle\bar{\nu}_F\rangle}{\bar{\nu}_0}-\Phi_T\frac{E_T}{hc\bar{\nu}_0}\right) \quad (20)$$

$$\left.\frac{H}{E}\right|_{R} = A(1-R) \quad (21)$$

where subscripts S and R denote sample and calorimetric reference respectively; A is an instrumental constant, function of the system geometry and the thermoelastic properties of the sample; R is the total reflectance at the laser (excitation) wavelength; $\langle\bar{\nu}_F\rangle$ is the average emission frequency; $\bar{\nu}_0$ is the excitation frequency; Φ_T is the triplet quantum yield and E_T is the triplet energy. If the same supporting material is used for the reference and the sample and both measurements are performed under the same conditions, then A is expected to be the same for sample and reference. Thus, this parameter can be obtained from the slope of the linear regression of H/E vs $(1 - R)$ for the calorimetric reference at different concentrations. Equation (20) is then used to calculate the fluorescence quantum yield if the triplet quantum yield is negligible, or the triplet quantum yield if the observed fluorescence quantum yield is known from a separate measurement.

EXPERIMENTAL RESULTS

Fluorescence quantum yields

The fluorescence quantum yield of hydroxoaluminum tricarboxymonoamidephthalocyanine (AlTCPc) adsorbed on microcrystalline cellulose was calculated as a function of the dye concentration from 0.02 to 2 μmol g^{-1} cellulose, obtaining Φ_{obs} values between 0.3 and 0.07 (48). The continuous decrease in Φ_{obs} with concentration was interpreted as a result of the filtering effect of and fluorescence reabsorption by phthalocyanine nonluminescent cofacial dimers. Evaluation of the aggregation degree was afforded through absorption spectral analysis. Calculation of Φ_F using an equation similar to Eq. (11) yielded a value of 0.46 ± 0.02 independent on concentration, near to the value found for the same phthalocyanine in DMSO solution, $\Phi_F = 0.42$. The fluorescence quantum yield in the solid is somewhat overestimated because it was assumed that $\Phi_{obs} = 1$ for the reference used, rhodamine 101 (R101). Later evaluation of the quantum yield of this compound on microcrystalline cellulose showed that it is lower than one and dependent on the location into the substrate (79).

In contrast, pheophorbide-a (Pheo) adsorbed on microcrystalline cellulose does not aggregate in a broader concentration range, 0.007–9 μmol g^{-1} cellulose, as demonstrated by the constancy of the shape of the remission function spectrum and the linearity of remission function with concentration (80). However, once corrected for reabsorption–reemission through Eq. (13), a strong decrease in Φ_F with concentration from 0.2 to 0.065 was observed, whereas the fluorescence quantum yield of this dye in methanol is 0.28. The important concentration quenching observed for Pheo was attributed to a Förster energy transfer and trapping mechanism. This conclusion was sustained by the fact that the fluorescence average lifetime was a decreasing function of concentration.

One argument in favor of the correction for reabsorption–reemission by Eq. (13) using calculated values of $\gamma(\lambda, \lambda_0)$ is the quasi independence on concentration of the emission spectrum $f(\lambda)$ obtained applying Eq. (9). In fact, an emission band with a constant shape is obtained in the above examples (48,80), but the position of the maximum suffers a slight bathochromic shift with concentration. The change in the emission maximum does not exceed 10 nm and is also found for thin layers of particles devoid of reabsorption–reemission effects. A similar behavior was observed for AlTCPc on silanized silica (81). This effect has been also found by others (62) and can be interpreted as a concentration-dependent Stokes shift due to the interaction of the excited state with neighbor ground-state molecules.

For rose bengal (RB) adsorbed on microcrystalline cellulose, application of Eq. (13) after quantification of the aggregation equilibrium yielded an apparent increase in Φ_F with concentration (49). This behavior cannot be explained unless dimer luminescence is considered in contradiction with the initial hypothesis. On extending the model to the case of two luminescent species, monomer and dimer fluorescence quantum yields were evaluated as 0.120 ± 0.004 and 0.070 ± 0.006 respectively. They may be compared with $\Phi_F = 0.11$ for monomeric RB in basic ethanol. Experimental results could therefore be explained considering a dimerization–reabsorption–reemission model with dimer emission and radiative energy transfer between monomers and dimers. The fact that, aside from hypochromism, no other changes in absorption spectra were observed on dimerization points to the occurrence of very weak interactions between monomers, consistent with the existence of luminescent dimers.

So far discussed examples show that the supporting material, microcrystalline cellulose, acts in all cases as an inert medium regarding monomer fluorescence spectra and quantum yields. Spectral shifts and small differences in quantum yields can be accounted for by the effect of polarity in the cellulose microenvironment. Aggregate formation arises either from the occurrence of ground-state interactions between dye molecules or as a result of increasing the concentrations in a restricted environment where dye molecules are distributed nearly at random, as it will be discussed later in this section.

Methylene blue (MB) forms nonfluorescent H-dimers even at 0.02 μmol g^{-1} when incorporated into cellulose (72). After considering aggregation–reabsorption–reemission effects through Eq. (13), a decrease in monomer fluorescence quantum yield on increasing concentration is still observed, suggesting the occurrence of nonradiative energy transfer from monomers to trapping dimers. In other cases concentration self-quenching takes place without spectroscopic evidence of dye aggregation as observed for Pheo on cellulose (80).

Concentration self-quenching can be explained quantitatively considering a FRET mechanism from monomers to energy trapping centers. Rhodamine 6G (R6G) adsorbed on microcrystalline cellulose does not show any spectroscopic evidence of dye aggregation between 0.02 and 4 μmol g^{-1} (70). However, after correction for reabsorption and reemission, a substantial decrease in Φ_F with concentration was observed. Shortening of fluorescence decays was also observed at the highest loadings. Quenching was then ascribed to R6G pairs (traps) that dissipate

excitation energy produced both by direct absorption (static quenching) and through nonradiative energy transfer from monomers (dynamic quenching). Trap concentrations were estimated considering two extreme approaches: a) traps are weakly interacting ground-state dimers showing spectral changes not detectable under the experimental conditions, whose concentration is related to a dimerization constant; and b) traps are molecular pairs located below a critical quenching distance interacting in the excited state (statistical pairs). Both approaches accounted quantitatively for the experimental results. The relative importance of energy migration was evaluated through computational simulations. From the statistical pairs approach a quenching radius of around 12–15 Å was obtained, in the order of molecular dimensions. This is compatible with quenching centers formed by slightly interacting molecules brought into close contact due to a random distribution of dye molecules at high local concentrations.

From these studies, a general view on molecular interaction effects on the photophysics of dyes in solid materials can be obtained. Short-range interactions lead to the formation of excitation energy traps (aggregates or statistical traps). Long-range interactions are responsible for resonance energy transfer, which accounts for self-quenching if the transfer occurs from monomers to traps. At even longer distances, interactions are responsible for concentration-dependent Stokes shifts (*vide supra*). A general scheme of molecular interaction effects is shown in Fig. 2 (71).

Donor–acceptor systems and light harvesting

Coadsorption is a known strategy to reduce dye aggregation (82). Probably due to the reduction in medium polarity, coadsorption of MB and Pheo, an hydrophobic dye, reduces the strong aggregation tendency of MB up to the point that no aggregates are found at concentrations as large as 1 μmol g^{-1} (72). In addition, Pheo has also an energy relay function. After excitation of Pheo, singlet excitation energy is conveyed both radiatively and nonradiatively to MB. Considering the model described in Fig. 1, a nonradiative energy transfer efficiency of nearly 40% was obtained at *ca* 1 μmol MB g^{-1}. At this concentration, MB fluorescence is mostly reabsorbed by the dye, repopulating the singlet state with the foreseeable result of enhancing triplet-state formation. The dependence of the energy transfer efficiency on MB concentration was modeled considering a random distribution of dyes and a FRET mechanism; see details in ref. (83).

For R101 chemically linked to cellulose and MB adsorbed on the same support, higher energy transfer efficiencies from R101 to MB were obtained: nearly 60% for nonradiative transfer and, for optically thick samples, almost 80% considering both radiative and nonradiative mechanisms at *ca* 1 μmol MB g^{-1} (84). In that case, the presence of R101 also reduced the aggregation tendency of MB. However, the dependence of energy transfer efficiencies on MB concentration showed deviations at lower concentrations from a model considering random distribution of dyes. Similar deviations were obtained for the R6G-MB system coadsorbed on cellulose (70) and for the dye pair 7-diethylamino-4-methylcoumarin (donor) to 3,3-dimethyloxacarbocyanine (acceptor) in polyvinyl alcohol films (85). In the last case, departures at low acceptor concentrations were attributed to energy migration between donor molecules. However, computational simulations of energy transfer considering energy migration with a Markovian model and random distribution of dyes (83) showed that departures cannot be ascribed to energy migration for R101-MB. Deviations were attributed in that case to a nonrandom distribution due to interactions between donor and acceptor molecules. These interactions are weak enough to cause undetectable spectroscopic changes by heteroaggregation, but strong enough to affect distribution of acceptors around donor molecules (70).

These studies helped in understanding the interplay between radiative and nonradiative mechanisms in light-scattering materials. As acceptor concentrations increase, reabsorption of donor fluorescence by the acceptor is enhanced for optically thick materials. However, in these conditions donor–acceptor average distances are low, favoring nonradiative transfer, which quenches donor fluorescence. Thus, radiative efficiencies reach a maximum at intermediate acceptor concentrations. In conditions where nonradiative energy transfer efficiencies are high, the contribution of trivial transfer is rather low.

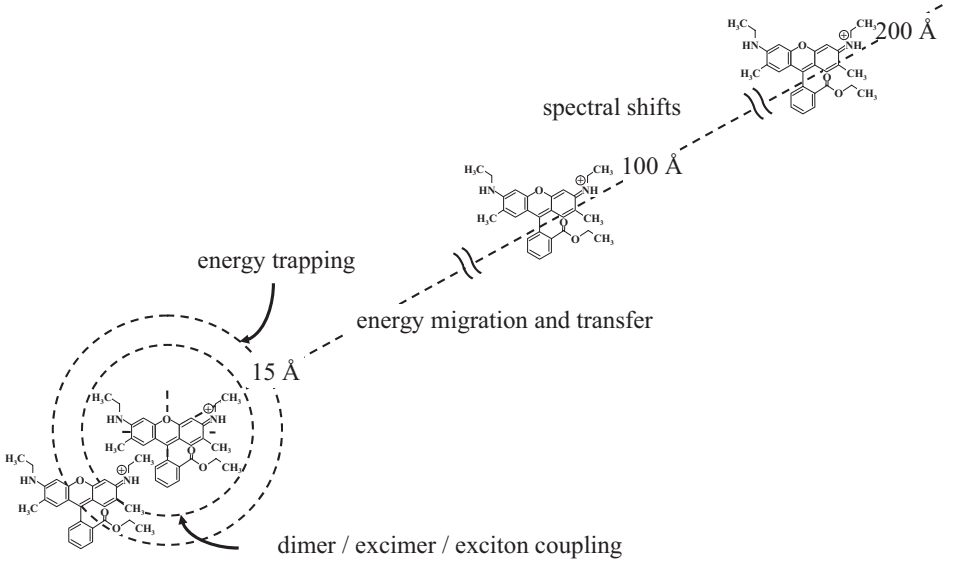

Figure 2. Interaction scheme illustrated for a R6G molecule (reprinted with permission from *Ann. N. Y. Acad. Sci.* **1130**, 247–252).

Determination of quantum yields by LIOAS

For highly fluorescent samples with negligible triplet quantum yield, as in the case of R6G and R101 adsorbed on microcrystalline cellulose, observed fluorescence quantum yields were determined by LIOAS, using Brilliant Blue G adsorbed on the same support as a calorimetric reference (77). These studies were performed to validate absolute fluorescence quantum yield determinations on optically thick light-scattering materials using reflectance spectroscopy, see Eq. (2). From the comparison of data obtained using both methods, the accuracy in Φ_{obs} values was established as ± 0.1.

Triplet quantum yield determinations were performed for RB and erythrosine B (EB) adsorbed on microcrystalline cellulose (78). These dyes are well-known Type-II photosensitizers, with Φ_T values nearby one in common solvents. Fluorescence quantum yields were determined in a relative way using R101 as the fluorescence reference, whose absolute quantum yield was previously obtained using LIOAS and reflectance measurements. Concentration-independent triplet quantum yields, $\Phi_T = 0.57 \pm 0.12$ and 0.55 ± 0.15, were obtained for RB and EB, respectively, lower than their values in water due to polarity effects. Adding up reabsorption-corrected monomer fluorescence quantum yields, values of $\Phi_F + \Phi_T = 0.70 \pm 0.13$ for RB and 0.72 ± 0.18 for EB were obtained. In contrast to water and alcohols, internal conversion cannot be neglected in cellulose, a poor electron donating medium. Strikingly, although significant fluorescence concentration quenching takes place, triplet quantum yields seem to be concentration independent up to concentrations in the order of 0.5 μmol g^{-1}.

The apparent independence of triplet quantum yields on concentration was attributed to a sort of compensation between the singlet decay pathways on aggregation. This matter is currently under study in our laboratory to unravel the singlet deactivation mechanisms in weakly interacting dimers or statistical traps.

CONCLUSIONS

Experimental methods based on measurements such as steady-state reflectance and fluorescence and LIOAS allow the quantitative evaluation of photophysical processes in light-scattering materials containing dyes at high loadings. Fluorescence and triplet quantum yield determinations as a function of dye concentration contribute to the study of self-quenching mechanisms by molecular aggregates or statistical traps leading to energy wasting and to the understanding of energy transfer processes in crowded dye systems. Energy transfer processes in donor–acceptor systems may be quantitatively evaluated through phenomenological models without any adjustable parameters. Results show that high transfer efficiencies can be achieved without any particular molecular organization. Considering the reduction in dye aggregation on coadsorption, it can be concluded that incorporation of energy relay dyes may be a good strategy to broaden absorption spectra, increasing light collection efficiency while reducing energy wasting due to self-quenching.

Acknowledgements—This work has been supported in part by the University of Buenos Aires (Grant 20020100100814) and CONICET (Grant PIP 112-200801-00319). H. B. R. and E. S. R. are staff members of CONICET.

AUTHOR BIOGRAPHIES

Hernán B. Rodríguez studied Biochemistry at the National University of Patagonia San Juan Bosco in Comodoro Rivadavia, República Argentina, obtaining his degree in 2001. Since 2004, through a fellowship from the National Scientific and Technological Research Council of Argentina (CONICET) he performed studies on the photophysics of dyes in heterogeneous systems at the Institute of Physical Chemistry of Materials, Environment and Energy (INQUIMAE) at the School of Sciences of the University of Buenos Aires, obtaining his PhD in Physical Chemistry in 2009. After a postdoctoral period at the same institution, he became Assistant Researcher of CONICET at the Research Institute of Theoretical and Applied Physical Chemistry (INIFTA) at the School of Sciences, University of La Plata, Argentina. Present research interests are nanoparticle-based and nanostructured photosensitizers, the photophysics and photochemistry of dyes in heterogeneous systems and the study of molecular interactions and energy and charge transfer processes.

Enrique San Román studied Chemistry at the University of Buenos Aires and moved to the National University of La Plata to perform PhD studies on the kinetics of gas-phase reactions, defending his Thesis at the University of Buenos Aires in 1977. He followed postdoctoral studies about reactions of solvated electrons at the University of Karlsruhe in Germany, returning to the University of La Plata until the middle 1980, when he moved again to the University of Buenos Aires. From the field of gaseous reactions he went into the photochemistry of dyes in solution and finally into the photochemistry of dyes in heterogeneous systems. After reaching the position of Full Professor in Chemistry at the School of Sciences of the University of Buenos Aires he has recently been designated as Consulting Professor at the same place. He belongs to the staff of the National Scientific and Technological Research Council of Argentina as Principal Researcher.

REFERENCES

1. Ricciardi, L., F. Puoci, G. Cirillo and M. La Deda (2012) A new member of the oxygen-photosensitizers family: A water-soluble polymer binding a platinum complex. *Dalton Trans.* **41**, 10923–10925.
2. Drozd, D., K. Szczubiałka and M. Nowakowska (2010) Novel hybrid photosensitizers: Photoactive polymer-nanoclay. *J. Photochem. Photobiol. A: Chem.* **215**, 223–228.
3. Suzuki, M., Y. Ohta, H. Nagae, T. Ichinohe, M. Kimura, K. Hanabusa, H. Shirai and D. Wöhrle (2000) Synthesis, characterization and application of a novel polymer solid photosensitizer. *Chem. Commun.* **3**, 213–214.

4. Lang, K., P. Bezdička, J. L. Bourdelande, J. Hernando, I. Jirka, E. Káfuňková, F. Kovanda, P. Kubát, J. Mosinger and D. M. Wagnerová (2007) Layered double hydroxides with intercalated porphyrins as photofunctional materials: Subtle structural changes modify singlet oxygen production. *Chem. Mater.* **19**, 3822–3829.
5. Hennig, A., S. Hatami, M. Spieles and U. Resch-Genger (2013) Excitation energy migration and trapping on the surface of fluorescent poly(acrylic acid)-grafted polymer particles. *Photochem. Photobiol. Sci.* **12**, 729–737.
6. Hungerford, G., J. Benesch, J. F. Mano and R. L. Reis (2007) Effect of the labelling ratio on the photophysics of fluorescein isothiocyanate (FITC) conjugated to bovine serum albumin. *Photochem. Photobiol. Sci.* **6**, 152–158.
7. Bae, B.-C. and K. Na (2012) Development of polymeric cargo for delivery of photosensitizer in photodynamic therapy. *Int. J. Photoenergy* **2012**, Art. ID 431975.
8. Park, W., S.-J. Park and K. Na (2011) The controlled photoactivity of nanoparticles derived from ionic interactions between a water soluble polymeric photosensitizer and polysaccharide quencher. *Biomaterials* **32**, 8261–8270.
9. Brühwiler, D. and G. Calzaferri (2004) Molecular sieves as host materials for supramolecular organization. *Microporous Mesoporous Mater.* **72**, 1–23.
10. Hardin, B. E., H. J. Snaith and M. D. McGehee (2012) The renaissance of dye-sensitized solar cells. *Nat. Photonics* **6**, 162–169.
11. Hardin, B. E., E. T. Hoke, P. B. Armstrong, J.-H. Yum, P. Comte, T. Torres, J. M. J. Fréchet, Md. K. Nazeeruddin, M. Grätzel and M. D. McGehee (2009) Increased light harvesting in dye-sensitized solar cells with energy relay dyes. *Nat. Photonics* **3**, 406–411.
12. Hoke, E. T., B. E. Hardin and M. D. McGehee (2010) Modeling the efficiency of Förster resonant energy transfer from energy relay dyes in dye-sensitized solar cells. *Opt. Express* **18**, 3893–3904.
13. Jonson, G. E., H. Fredriksson, R. Sellappan and D. Chakarov (2011) Nanostructures for enhanced light absorption in solar energy devices. *Int. J. Photoenergy*, **2011**, Art. ID 939807.
14. Martini, M., M. Montagna, M. Ou, O. Tillement, S. Roux and P. Perriat (2009) How to measure quantum yields in scattering media: Application to the quantum yield measurement of fluorescein molecules encapsulated in sub-100 nm silica particles. *J. Appl. Phys.* **106**, 94304.
15. Gaigalas, A. K. and L. Wang (2008) Measurement of the fluorescence quantum yield using a spectrometer with an integrating sphere detector. *J. Res. Natl. Inst. Stand. Technol.* **113**, 17–28.
16. Gaigalas, A. K., H.-J. He and L. Wang (2009) Measurement of absorption and scattering with an integrating sphere detector: Application to microalgae. *J. Res. Natl. Inst. Stand. Technol.* **114**, 69–81.
17. Botehlo do Rego, A. M. and L. F. Vieira Ferreira (2001) Photonic and electronic spectroscopies for the characterization of organic surfaces and organic molecules adsorbed on surfaces. In *Handbook of Surfaces and Interfaces of Materials*, Ch. 7, Vol. II (Edited by H. S. Nalga), pp. 275–313. Acad. Press, San Diego.
18. Demas, J. N. and G. A. Crosby (1971) The measurement of photoluminescence quantum yields. A review. *J. Phys. Chem.* **75**, 991–1024.
19. Braslavsky, S. E. (2007) Glossary of terms used in photochemistry, 3rd edn. (IUPAC Recommendations 2006). *Pure Appl. Chem.* **79**, 293–465.
20. Valeur, B. (2001) *Molecular Fluorescence: Principles and Applications*. Wiley-VCH Verlag GmbH, Weinheim.
21. Vieira Ferreira, L. F., S. M. B. Costa and E. J. Pereira (1991) Fluorescence quantum yield evaluation of strongly absorbing dye solutions as a function of the excitation wavelength. *J. Photochem. Photobiol. A* **55**, 361–376.
22. Birks, J. B. (1976) Fluorescence quantum yield measurements. *J. Res. Natl. Bureau Standards A: Phys. Chem.* **80A**, 389–399.
23. Wrighton, M. S., D. S. Ginley and D. L. Morse (1974) A technique for the determination of absolute emission quantum yields of powdered samples. *J. Phys. Chem.* **78**, 2229–2233.
24. Liu, Y. S., P. de Mayo and W. R. Ware (1993) Photophysics of polycyclic aromatic hydrocarbons adsorbed on silica gel surfaces. 3. Fluorescence quantum yields and radiative decay rate constants derived from lifetime distributions. *J. Phys. Chem.* **97**, 5995–6001.
25. Wendlandt, W. W. and H. G. Hecht (1966) *Reflectance Spectroscopy*, Ch. 3, pp. 55–76. Wiley Interscience, New York.
26. de Mello, J. C., H. F. Wittmann and R. H. Friend (1997) An improved experimental determination of external photoluminescence quantum efficiency. *Adv. Mat.* **3**, 230–232.
27. Mirenda, M., M. G. Lagorio and E. San Román (2004) Photophysics on surfaces: Determination of absolute fluorescence quantum yields from reflectance spectra. *Langmuir* **20**, 3690–3697.
28. Vieira Ferreira, L. F., T. J. F. Branco and A. M. Botelho do Rego (2004) Luminescence quantum yield determination for molecules adsorbed onto solid powdered particles. *Chem. Phys. Chem.* **5**, 1848–1854.
29. Plant, A. L. (1986) Mechanism of concentration quenching of a xanthene dye encapsulated in phospholipid vesicles. *Photochem. Photobiol.* **44**, 453–459.
30. Chen, R. F. and J. R. Knutson (1988) Mechanism of fluorescence concentration quenching of carboxyfluorescein in liposomes: Energy transfer to nonfluorescent dimers. *Anal. Biochem.* **172**, 61–77.
31. Razumov, V. F. and A. G. Ivanchenko (1995) Concentration fluorescence quenching of cyanine dyes in micellar solutions and microemulsions. *Opt. Spectrosc.* **79**, 568–573.
32. Martini, M., P. Perriat, M. Montagna, R. Pansu, C. Julien, O. Tillement and S. Roux (2009) How gold particles suppress concentration quenching of fluorophores encapsulated in silica beads. *J. Phys. Chem. C* **113**, 17669–17677.
33. Konan, Y. N., R. Gurny and E. Allémann (2002) State of the art in the delivery of photosensitizers for photodynamic therapy. *J. Photochem. Photobiol. B* **66**, 89–106.
34. Bechet, D., P. Couleaud, C. Frochot, M.-L. Viriot, F. Guillemin and M. Barberi-Heyob (2008) Nanoparticles as vehicles for delivery of photodynamic therapy agents. *Trends Biotechnol.* **26**, 612–621.
35. Chen, W. (2008) Nanoparticle fluorescence based technology for biological applications. *J. Nanosci. Nanotechnol.* **8**, 1019–1051.
36. Martínez Martínez, V., F. López Arbeloa, J. Bañuelos Prieto and I. López Arbeloa (2005) Characterization of rhodamine 6G aggregates intercalated in solid thin films of laponite clay. 2 Fluorescence spectroscopy. *J. Phys. Chem. B* **109**, 7443–7450.
37. Deshpande, A. V. and E. B. Namdas (2000) Correlation between lasing and photophysical performance of dyes in polymethylmethacrylate. *J. Lumin.* **91**, 25–31.
38. Bojarski, P. (1997) Concentration quenching and depolarization of rhodamine 6G in the presence of fluorescent dimers in polyvinyl alcohol films. *Chem. Phys. Lett.* **278**, 225–232.
39. Anfinrud, P. A., T. P. Causgrove and W. S. Struve (1986) Picosecond pump-probe experiments on surface-adsorbed dyes: Ground-state recovery of Rhodamine 640 on zinc oxide and fused silica. *J. Phys. Chem.* **90**, 5887–5891.
40. Tamai, N., T. Yamazaki and I. Yamazaki (1988) Excitation energy relaxation of rhodamine B in Langmuir–Blodgett monolayer films: Picosecond time-resolved fluorescence studies. *Chem. Phys. Lett.* **147**, 25–29.
41. Vuorimaa, E., M. Ikonen and H. Lemmetyinen (1994) Photophysics of rhodamine dimers in Langmuir–Blodgett films. *Chem. Phys.* **188**, 289–302.
42. Pevenage, D., M. Van der Auweraer and F. C. De Schryver (1999) Influence of the molecular structure on the lateral distribution of xanthene dyes in Langmuir–Blodgett films. *Langmuir* **15**, 8465–8473.
43. Ballet, P., M. Van der Auweraer, F. C. De Schryver, H. Lemmetyinen and E. Vuorimaa (1996) Global analysis of the fluorescence decays of N,N′-dioctadecyl rhodamine B in Langmuir–Blodgett films of diacylphosphatidic acids. *J. Phys. Chem.* **100**, 13701–13715.
44. Birks, J. B. (1970) *Photophysics of Aromatic Molecules*. Wiley-Interscience, London.
45. Demchenko, A. P. (2002) The red-edge effects: 30 years of exploration. *Luminescence* **17**, 19–42.
46. Oelkrug, D. and G. Kortüm (1968) Zur Berechnung der Lumineszenzreabsorption by pulverförmigen Substanzen. *Z. Physik. Chemie N. F.* **58**, 181–188.
47. Wilkinson, F. and G. P. Kelly (1989) Diffuse reflectance flash photolysis. In *Handbook of Organic Photochemistry*, Vol. I (Edited by J. C. Scaiano), pp. 293–314. CRC Press, Boca Raton.
48. Lagorio, M. G., L. E. Dicelio, M. I. Litter and E. San Román (1998) Modeling of fluorescence quantum yields of supported dyes. Aluminum carboxyphthalocyanine on cellulose. *J. Chem. Soc. Faraday Trans.* **94**, 419–425.

49. Rodríguez, H. B., M. G. Lagorio and E. San Román (2004) Rose bengal adsorbed on microgranular cellulose: Evidence on fluorescent dimers. *Photochem. Photobiol. Sci.* **3**, 674–680.
50. Beddard, G. S. and G. Porter (1976) Concentration quenching in chlorophyll. *Nature* **260**, 366–367.
51. Boulu, L. G., L. K. Patterson, J. P. Chauvet and J. J. Kozak (1987) Theoretical investigation of fluorescence concentration quenching in two-dimensional disordered systems. Application to chlorophyll a in monolayers of dioleylphosphatidylcholine. *J. Chem. Phys.* **86**, 503–507.
52. Knoester, J. and J. E. Van Himbergen (1987) On the theory of concentration self-quenching by statistical traps. *J. Chem. Phys.* **86**, 3571–3576.
53. Dahim, M., N. K. Mizuno, X.-M. Li, W. E. Momsen, M. M. Momsen and H. L. Brockman (2002) Physical and photophysical characterization of a BODIPY phosphatidylcholine as a membrane probe. *Biophys. J.* **83**, 1511–1524.
54. Juzeliūnas, G. and D. L. Andrews (1999) Unified theory of radiative and radiationless energy transfer. In *Resonance Energy Transfer* (Edited by D. L. Andrews and A. A. Demidov), pp. 65–107. Wiley, Chichester.
55. Scholes, G. D. (2003) Long-range resonance energy transfer in molecular systems. *Annu. Rev. Phys. Chem.* **54**, 57–87.
56. Kasha, M. (1963) Energy transfer mechanisms and the molecular exciton model for molecular aggregates. *Radiat. Res.* **20**, 55–71.
57. Kasha, M., H. R. Rawls and M. Ashraf El-Bayoumi (1965) The exciton model in molecular spectroscopy. *Pure Appl. Chem.* **11**, 371–391.
58. Förster, Th. (1959) Transfer mechanisms of electronic excitation. *Discuss. Faraday Soc.* **27**, 7–17.
59. Braslavsky, S. E., E. Fron, H. B. Rodríguez, E. San Román, G. D. Scholes, G. Schweitzer, B. Valeur and J. Wirz (2008) Pitfalls and limitations in the practical use of Förster's theory of resonance energy transfer. *Photochem. Photobiol. Sci.* **7**, 1444–1448.
60. Förster, Th. (1949) Experimentelle und Theoretische Untersuchung des zwischenmolekularen Übergangs von Elektronenanregungsenergie. *Z. Naturforsch.* **4a**, 321–327.
61. Fung, B. K.-K. and L. Stryer (1978) Surface density determination in membranes by fluorescence energy transfer. *Biochemistry* **17**, 5241–5248.
62. Itoh, K., Y. Chiyokawa, M. Nakao and K. Honda (1984) Fluorescence quenching processes of Rhodamine B on oxide semiconductors and light-harvesting action of its dimers. *J. Am. Chem. Soc.* **106**, 1620–1627.
63. Huber, D. L. (1979) Fluorescence in the presence of traps. *Phys. Rev. B* **20**, 2307–2314.
64. Gouchanour, C. R., H. C. Anderson and M. D. Fayer (1979) Electronic excited state transport in solution. *J. Chem. Phys.* **70**, 4254–4271.
65. Loring, R. F., H. C. Anderson and M. D. Fayer (1982) Electronic excited state transport and trapping in solution. *J. Chem. Phys.* **76**, 2015–2027.
66. Kulak, L. and C. Bojarski (1995) Forward and reverse electronic energy transport and trapping in solution. I. Theory. *Chem. Phys.* **191**, 43–66.
67. Engström, S., M. Lindberg and L. B.-Å. Johansson (1988) Monte Carlo simulations of electronic energy transfer in three-dimensional systems: A comparison with analytical theories. *J. Chem. Phys.* **89**, 204–213.
68. Kulak, L. and C. Bojarski (1995) Forward and reverse electronic energy transport and trapping in solution. II. Numerical results and Monte Carlo simulations. *Chem. Phys.* **191**, 67–86.
69. Carlsson, C., A. Larsson, M. Björkman, M. Jonsson and B. Albinsson (1997) Experimental and simulated fluorescence depolarization due to energy transfer as tools to study DNA-dye interactions. *Biopolymers* **41**, 481–494.
70. López, S. G., G. Worringer, H. B. Rodríguez and E. San Román (2010) Trapping of Rhodamine 6G excitation energy on cellulose microparticles. *Phys. Chem. Chem. Phys.* **12**, 2246–2253.
71. Rodríguez, H. B. and E. San Román (2008) Excitation energy transfer and trapping in dye-loaded solid particles. *Ann. N. Y. Acad. Sci.* **1130**, 247–252.
72. Rodríguez, H. B., A. Iriel and E. San Román (2006) Energy transfer among dyes on particulate solids. *Photochem. Photobiol.* **82**, 200–207.
73. Tam, A. C. (1986) Applications of photoacoustic sensing techniques. *Rev. Mod. Phys.* **58**, 381–431.
74. Peters, K. S. (1986) Time-resolved photoacoustic calorimetry. *Pure Appl. Chem.* **58**, 1263–1266.
75. Braslavsky, S. E. and G. E. Heibel (1992) Time-resolved photothermal and photoacoustic methods applied to photoinduced processes in solution. *Chem. Rev.* **92**, 1381–1410.
76. Gensch, T., C. Viappiani and S. E. Braslavsky (1999) Laser-induced time-resolved optoacoustic spectroscopy in solution. In *Encyclopedia of Spectroscopy and Spectrometry* (Edited by J. C. Lindon, G. E. Tranter and J. L. Holmes), pp. 1124–1132. Academic Press, London.
77. Tomasini, E. P., E. San Román and S. E. Braslavsky (2009) Validation of fluorescence quantum yields for light-scattering powdered samples by laser-induced optoacoustic spectroscopy. *Langmuir* **25**, 5861–5868.
78. Tomasini, E. P., S. E. Braslavsky and E. San Román (2012) Triplet quantum yields in light-scattering powder samples measured by laser-induced optoacoustic spectroscopy (LIOAS). *Photochem. Photobiol. Sci.* **11**, 1010–1017.
79. Iriel, A. (2006) Fotofísica de colorantes inmovilizados sobre superficies. Ph.D thesis, University of Buenos Aires.
80. Lagorio, M. G., E. San Román, A. Zeug, J. Zimmermann and B. Röder (2001) Photophysics on surfaces: Absorption and luminescence properties of pheophorbide-a on cellulose. *Phys. Chem. Chem. Phys.* **3**, 1524–1529.
81. Iriel, A., M. G. Lagorio, L. E. Dicelio and E. San Román (2002) Photophysics of supported dyes: Phthalocyanine on silanized silica. *Phys. Chem. Chem. Phys.* **4**, 224–231.
82. Amao, Y. and T. Komori (2003) Dye-sensitized solar cell using a TiO_2 nanocrystalline film electrode modified by an aluminum phthalocyanine and myristic acid coadsorption layer. *Langmuir* **19**, 8872–8875.
83. Rodríguez, H. B. (2009) Fotofísica de colorantes sobre sólidos particulados: interacciones moleculares y transferencia de energía. Ph.D thesis, University of Buenos Aires.
84. Rodríguez, H. B. and E. San Román (2007) Energy transfer from chemically attached rhodamine 101 to adsorbed methylene blue on microcrystalline cellulose particles. *Photochem. Photobiol.* **83**, 547–555.
85. Tripathy, U. and P. B. Bishta (2006) Effect of donor-acceptor interaction strength on excitation energy migration and diffusion at high donor concentrations. *J. Chem. Phys.* **125**, 144502.